

## **THE PHYSICAL AND MATHEMATICAL MODELLING OF PLASTIC DEFORMATION OF SAMPLES WITH MUSHY ZONE**

**Mirosław Glowacki**

*Department of Computer Science in Industry  
AGH University of Science and Technology  
Krakow Poland  
glowacki@metal.agh.edu.pl*

**Marcin Hojny**

*Department of Computer Science in Industry  
AGH University of Science and Technology  
Krakow Poland  
mhojny@metal.agh.edu.pl*

**Zbigniew Malinowski**

*Department of Heat Engineering and  
Environmental Protection  
AGH University of Science and Technology  
Krakow Poland  
malinows@metal.agh.edu.pl*

**Dariusz Jędrzejczyk**

*Department of Computer Science in Industry  
AGH University of Science and Technology  
Krakow Poland  
djedrzej@metal.agh.edu.pl*

### **ABSTRACT**

The subject of the presented paper is the modelling of steel behaviour in temperature which exceeds the hot rolling temperature range. The inverse method, which is usually applied for calculation of real strain-stress relationship needs good mathematical model describing the plastic behaviour of the material. The inspiration of the presented work was the lack of models allowing the numerical analysis of compression test in case of samples, which still have the liquid phase in their central parts and show extremely high strain inhomogeneity. The paper reports the results of experimental and theoretical work leading to construction of an appropriate mathematical model describing the phenomena accompanying the deformation in temperatures which are characteristic for direct rolling of continuously cast charge.

A coupled thermal-mechanical mathematical model was used for simulation of plastic behaviour of a steel specimen. The model has been developed by authors for simulation of processes which require high accuracy required by the inverse method. The incompressibility condition and controlled compressibility is introduced to the model in analytical form. It can avoid problems with unintentional specimen volume changes. It is important in modelling of thermo-mechanical behaviour of steel samples in temperature range which is characteristic for the transformation of state of aggregation. Existing steel density changes in the mushy zone can cause volume variations close to those which are coming from numerical errors. In the present

work the application of the model to simulation of plastic behaviour of steel samples is presented together with material properties in temperature range between liquidus and solidus.

Although the current paper summarises the experimental work as well, first of all it reports the results of calculations according to mathematical model describing the phenomena accompanying the deformation at temperatures which are characteristic to rolling of continuously cast billets or slabs directly after casting. The model was applied for simulation of deformation of cylindrical samples, which are usually used for laboratory tests on GLEEBLE 3800 simulator.

### **INTRODUCTION**

In the course of experimental work carried out using GLEEBLE 3800 simulator the samples were subjected to the plastic deformation at temperatures which were higher than the solidus temperature. The plastic behaviour of such a specimen with mushy zone differs from the deformation of solid metal. During the successive drop in specimen temperature the thickness of the solid shell grows and the material becomes more and more stress resistant.

The material behaviour above the solidus line is strongly temperature-dependent. There are a few characteristic temperature values between solidus and liquidus [1,2]. The nil strength temperature (NST) is the temperature in which material strength drops to zero while the steel is being heated above the solidus temperature. Another temperature, which is associated with

NST, is the strength recovery temperature (SRT), which is specified during cooling. At this temperature the material regains strength greater than  $0,5 \text{ N/mm}^2$ . Nil ductility temperature (NDT) represents the temperature at which the heated material losses its ductility. The ductility recovery temperature (DRT) is the temperature at which the ductility of the material characterised by reduction of area reaches 5% while it is being cooled. Below this temperature plastic deformation is allowed.

Very important for plastic behaviour is also the material density. It varies with temperature and depends on the cooling rate. The solidification process causes non-uniform density distribution in the controlled volume. There are three main factors causing density changes: solid phase formation, thermal shrinkage and liquid movement inside the mushy zone. The density plays an important role in both mechanical and thermal solutions.

One of the most important relationships having crucial influence on the metal flow path is the strain-stress curve. It is not easy to construct the isothermal curves for a selected temperature range. Keeping constant temperature during the experiment is difficult. There are some difficulties with interpretation of measurements. Lack of good methods of simulation of metal flow and significant inhomogeneity in strain distribution in the deformation zone leads to weak accuracy in stress field determination. The model presented in the current paper fills the gap in modelling of plastic deformation of semi-solid materials.

### **MATHEMATICAL MODEL**

The mathematical model of the process consists of two main parts. The mechanical part is responsible for the strain, strain rate and stress distribution in a controlled volume. The stress due to shrinkage and plastic deformation is substantial. It can cause cracks in case the stress exceeds the ultimate tensile strength, which is low within discussed temperature range.

Thermal solution has crucial influence on simulation results, since the temperature has strong effect on remaining variables. Plastic flow of solid and porous materials, stress distribution and density changes are relevant to the temperature field, especially for deformation of body which consist of solid and mushy zones.

The analysis of possible models which can be applied for stress calculations for the discussed process has proved good predictive ability of a rigid-plastic model of metal flow. The model is completed with numerical solution of Navier

stress equilibrium equations. Such a model was selected due to its very good accuracy with reference to strain field during the hot deformation and sufficient correctness of calculated stress field [4]. Classical rigid-plastic solutions are based on optimisation of power functional.

$$J^*[v(r, z)] = W_\sigma + W_\lambda + W_f \quad (1)$$

where  $W_\sigma$  is the plastic deformation power,  $W_\lambda$  the penalty for the departure from the incompressibility or controlled compressibility conditions and  $W_f$  the friction power. In presented solution the second part of functional (1) is missing and both incompressibility and controlled compressibility conditions are given in analytical form and constrain the velocity field components. The functional takes the following shape:

$$J^*[v(r, z)] = W_\sigma + W_f \quad (2)$$

where  $v$  describes the velocity field distribution in the deformation zone. The optimisation of the functional (2) is much easier than the functional (1), because numerical form of incompressibility condition generates a lot of local minimums and leads to wide flat neighbourhood of the global optimum. The accuracy of the proposed solution is much better because of minimal volume lost. This is important for materials with changing density. In classical solutions the numerical errors which are caused by volume lost can be comparable with those coming from density changes. All that leads to solution with low accuracy contrary to the model with analytical incompressibility condition.

For solid regions of the sample the incompressibility condition in cylindrical coordinate system has been described with an equation:

$$\frac{\partial v_r}{\partial r} + \frac{v_r}{r} + \frac{\partial v_z}{\partial z} = 0 \quad (3)$$

where  $v_r$  and  $v_z$  are the velocity field components in cylindrical coordinate system  $r, \theta, z$ . For the mushy zone equation (3) is replaced by the controlled compressibility condition, which takes a form:

$$\frac{\partial v_r}{\partial r} + \frac{v_r}{r} + \frac{\partial v_z}{\partial z} - \frac{1}{\rho} \frac{\partial \rho}{\partial \tau} = 0 \quad (4)$$

where  $\rho$  is the temporary material density and  $\tau$  – the time variable.

Both the strain and stress models are based on Levy-Mises flow criterion

$$s_{ij} = \frac{2}{3} \frac{\sigma_p}{\dot{\epsilon}_i} \dot{\epsilon}_{ij} \quad (5)$$

As mentioned before, the velocity field has to satisfy either the incompressibility or controlled compressibility condition given in analytical form. A new local coordinate system was applied. The local coordinates depend on the functions describing the boundary of the deformation zone, i.e.  $h_1 = h_1(r)$  and  $h_2 = h_2(r)$ :

$$\begin{aligned} x &= \frac{r}{R_m} \\ y &= \frac{2z - h_2 - h_1}{h_2 - h_1} \end{aligned} \quad (6)$$

In elementar local region the radial velocity has a shape:

$$v_r = \frac{1}{2} \frac{rv_0}{h_2 - h_1} \left( 1 + \frac{\partial W}{\partial y} \right) \quad (7)$$

where  $W = W(x, y)$  is a function of velocity field components distribution in local coordinate system. Equation (7) can be differentiated with respect to  $r$  coordinate. It results in following equation

$$\begin{aligned} \frac{\partial v_r}{\partial r} &= \frac{v_0}{2\Delta h} \left( 1 + \frac{\partial W}{\partial y} + x \frac{\partial^2 W}{\partial x \partial y} \right) - \frac{rv_0 h_{r-}}{2(\Delta h)^2} \\ &\quad \left[ 1 + \frac{\partial W}{\partial y} + \frac{\partial^2 W}{\partial y^2} \left( \frac{h_{r+}}{h_{r-}} + y \right) \right] \end{aligned} \quad (8)$$

where

$$\begin{aligned} h_{r+} &= \frac{\partial h_2}{\partial r} + \frac{\partial h_1}{\partial r} \\ h_{r-} &= \frac{\partial h_2}{\partial r} - \frac{\partial h_1}{\partial r} \\ \Delta h &= h_2 - h_1 \end{aligned} \quad (9)$$

Taking into account condition (4), which is more general than relationship (3) the first derivative of velocity  $v_z$  with respect to  $z$  coordinate can be calculated according to the following formula:

$$\frac{\partial v_z}{\partial z} = -\frac{\partial v_r}{\partial r} - \frac{v_r}{r} + \frac{1}{\rho} \frac{\partial \rho}{\partial \tau} \quad (10)$$

Existing in the relationship (10)  $v_r$  and its derivative can be substitute by relationships (7) and (8). After subsequent integration the result leads to general shape of  $v_z$  velocity distribution.

$$\begin{aligned} v_z &= \frac{rv_0}{4} \frac{h_{r-}}{\Delta h} \left[ \frac{2z}{\Delta h} + \left( 1 - \frac{\Delta h}{2} \right) W + \right. \\ &\quad \left. + \left( \frac{h_{r+}}{h_{r-}} + y \right) \frac{\partial W}{\partial y} \right] - \\ &\quad - \frac{v_0}{4} \left[ \frac{2z}{\Delta h} + 2W + x \frac{\partial W}{\partial x} \right] + \frac{z}{\rho} \frac{\partial \rho}{\partial \tau} \end{aligned} \quad (11)$$

The velocity field, which is described by equations (7) and (11), satisfies the controlled compressibility condition. More details concerning the presented kinematical model but for bodies without density changes was published in [5].

The Navier equations, which complete the solution, are given in a form

$$\begin{aligned} \frac{\partial \sigma_{rr}}{\partial r} + \frac{\partial \sigma_{rz}}{\partial z} + \frac{\sigma_{rr} - \sigma_{\theta\theta}}{\partial r} &= 0 \\ \frac{\partial \sigma_{rz}}{\partial r} + \frac{\sigma_{rz}}{\partial r} + \frac{\partial \sigma_{zz}}{\partial z} &= 0 \end{aligned} \quad (12)$$

In equation (5)  $s_{ij}$  represents the stress deviator components,  $\sigma_p$  the field stress,  $\dot{\epsilon}_i$  the effective strain rate and  $\dot{\epsilon}_{ij}$  the strain rate tensor components. Replacement existing in equation set (12) components of the stress tensor  $\sigma_{rr}$ ,  $\sigma_{zz}$ ,  $\sigma_{\theta\theta}$  and  $\sigma_{rz}$  with relationships:

$$\begin{aligned} \sigma_{rr} &= s_{rr} + \sigma_m \\ \sigma_{zz} &= s_{zz} + \sigma_m \\ \sigma_{\theta\theta} &= s_{\theta\theta} + \sigma_m \\ \sigma_{rz} &= s_{rz} \end{aligned} \quad (13)$$

and comparison of the left sides of equations (12) leads to following differential equation

$$\begin{aligned} \frac{\partial \sigma_m}{\partial r} - \frac{\partial \sigma_m}{\partial z} &= F(r, z) = \\ &= \frac{\partial s_{rz}}{\partial r} + \frac{s_{rz}}{r} + \frac{\partial s_{zz}}{\partial z} - \frac{\partial s_{rr}}{\partial r} - \frac{\partial s_{rz}}{\partial z} - \frac{s_{rr} - s_{\theta\theta}}{r} \end{aligned} \quad (14)$$

Replacement of the stress tensor components in equation (14) with strain rate tensor components according to the equation (5) leads to new shape of the function  $F$

$$F(r, z) = \frac{2}{3} \left[ \frac{\sigma_p}{\dot{\epsilon}_i} a + b + c \right] \quad (15)$$

where  $a, b, c$  are given by following equations:

$$a = \frac{\partial \dot{\epsilon}_{zz}}{\partial z} - \frac{\partial \dot{\epsilon}_{rz}}{\partial z} + \frac{\partial \dot{\epsilon}_{rz}}{\partial r} - \frac{\partial \dot{\epsilon}_{rr}}{\partial r} + \frac{\dot{\epsilon}_{rz} - \dot{\epsilon}_{rr} + \dot{\epsilon}_{\theta\theta}}{r} \quad (16)$$

$$b = \left( \frac{\dot{\epsilon}_{zz}}{\dot{\epsilon}_i} - \frac{\dot{\epsilon}_{rz}}{\dot{\epsilon}_i} \right) \left( \frac{\partial \sigma_p}{\partial z} - \frac{\sigma_p}{\dot{\epsilon}_i} \frac{\partial \dot{\epsilon}_i}{\partial z} \right) \quad (17)$$

$$c = \left( \frac{\dot{\epsilon}_{rz}}{\dot{\epsilon}_i} - \frac{\dot{\epsilon}_{rr}}{\dot{\epsilon}_i} \right) \left( \frac{\partial \sigma_p}{\partial r} - \frac{\sigma_p}{\dot{\epsilon}_i} \frac{\partial \dot{\epsilon}_i}{\partial r} \right) \quad (18)$$

The optimisation of functional (1) delivers the velocity field in the deformation zone. It allows to find the solution of the differential equation (15) together with appropriate boundary conditions. As a result the mean stress  $\sigma_m$  can be calculated as well as the full stress tensor (the components of its deviatoric part are calculated according to the Levy-Mises law).

The temperature field is a solution of Fourier-Kirchhoff equation with convection. The most general form of this equation can be written as:

$$\nabla^T (k \nabla T) + \left[ Q - c \rho \left( \frac{\partial T}{\partial \tau} + v \circ \nabla T \right) \right] = 0 \quad (19)$$

where  $T$  is the temperature distribution in the controlled volume,  $k$  denotes the isotropic heat conduction coefficient,  $Q$  represents the rate of heat generation due to the plastic work done and  $c$  describes the specific heat. The solution of equation (19) has to satisfy the boundary conditions. The combined Hankel's boundary conditions have been adopted for the presented model.

$$k \frac{\partial T}{\partial n} + \alpha(T - T_0) + q = 0 \quad (20)$$

In equation (20)  $T_0$  is the distribution of the border temperature,  $q$  describes the heat flux through the boundary of the deformation zone,  $\alpha$  is the heat transfer coefficient and  $n$  is the normal to the boundary surface.

One of the most important parameters of the solution is the density. Its changes have influence on the mechanical part of the presented model.

The knowledge of effective density distribution is very important for modelling the deformation of porous materials. Density changes of liquid, solid-liquid and solid materials are ruled over three phenomena: solid phase formation, laminar liquid flow through porous material and thermal shrinkage. Total density changes can be calculated according to following equation:

$$\begin{aligned} \frac{\partial \rho}{\partial \tau} = & (\rho_s X_s + \rho_l X_l) \left( \frac{\rho_s}{\rho_l} - 1 \right) \frac{\partial X_l}{\partial \tau} + \\ & + \rho_l X_l \operatorname{div} v + \\ & + (\beta_s \rho_s X_s + \beta_l \rho_l X_l) \frac{\partial T}{\partial \tau} \end{aligned} \quad (21)$$

where  $X$  is the fraction and  $\beta$  the linear expansion coefficient. Indexes  $l$  and  $s$  denote the liquid and solid phases, respectively.

Another possibility of description of the density changes has been presented in paper [6]. The authors have presented dependence of density on temperature for a set of steel grades. In Fig. 1 such a graph concerning steel with carbon content of 0.11% is presented.

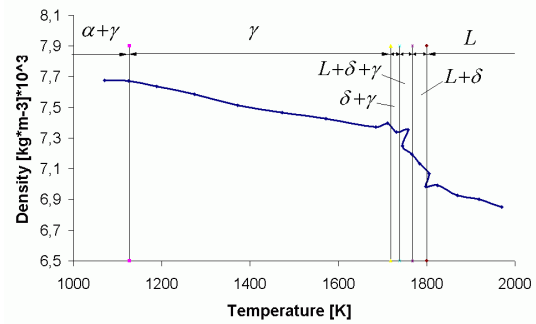


Fig. 1. The density versus temperature

The idea of calculation of density changes taking into account the experimental data leads to slightly less accurate results but such a method makes easier the solution. The last conception was applied in the presented mathematical model.

## EXPERIMENTAL WORK

The experimental work was done in Institute for Ferrous Metallurgy in Gliwice, Poland. In Fig. 2 the shape of the tested samples and locations of thermocouples are shown. The testing material was the BW11 grade steel investigated using GLEEBLE 3800 physical simulator.

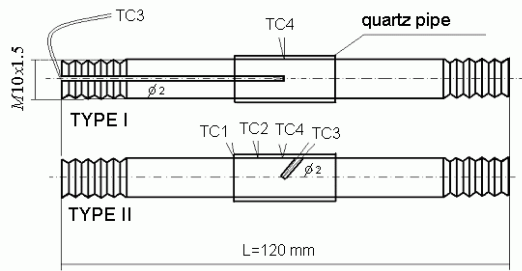


Fig. 2. Samples used during the experiments. TC1 ÷ TC4 – thermocouples

The chemical composition of the steel is given in Table 1. The liquidus temperature of BW11 grade steel is 1523°C. The average NST temperature for the selected steel was 1447°C.

Table 1. The chemical composition of the investigated steel

Element content (in mass%)						
C	Mn	Si	P	S	Cr	Ni
0.096	0.35	0.13	0.009	0.005	0.03	0.07
Cu	Sn	Al	Ti	Ca	N	
0.15	0.015	0.036	0.025	0.0026	0.008	

In aim to determine the nil ductility temperature (NDT) a number of experiments were done. All the tests lead to common temperature of 1420°C. The estimated ductility recovery temperature was 1385°C. At this temperature the sample's reduction of area was around 5% and rose very fast with the temperature drop. The strain-stress curves, which are necessary for the mechanical model, were constructed on basis of a series of experiments conducted on GLEEBLE simulator, as well [7]. Fig. 3 shows the relationships for 1300°C, 1375°C and 1420°C.

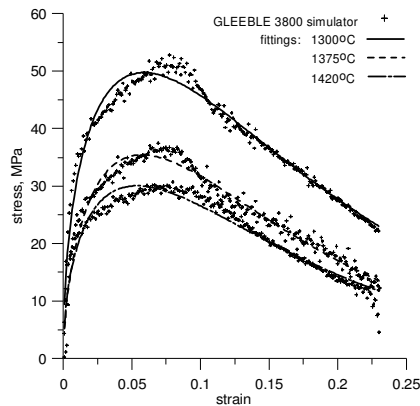


Fig. 3. Strain-stress relationship curves

Fig 3 includes results of measurements (the points in the form of symbol '+') and curves, which are the results of approximation of experiental data. The approximated curves are described by following equation:

$$\sigma = a\varepsilon^b \exp(c\varepsilon) \quad (22)$$

where  $a$ ,  $b$  and  $c$  are the coefficients calculated by approximation of the experimental data. They are collected in Table 2.

Table 2. The coefficients of the strain-stress curves

T [oC]	a	b	c
1300	336.7	0.499	-8.47
1375	348.2	0.592	-10.31
1420	223.3	0.511	-9.53

While making the analysis of the curves one can notice that the theoretical curves fit the experimental data well for all the testing temperatures. For this reason the curves approximated using the equation (22) with coefficients collected in Table 2 were used in the model of compression of sample with mushy core.

## RESULTS

An example simulation of compression of cylindrical samples, which are presented in Fig. 2 has been performed. The results of the test demonstrate the possibilities of the presented model. The initial temperature distribution in the deformation zone was calculated in such a manner that the computed temperatures in locations of thermocouples shown in Fig. 2 were consistent with their measured values. The simulation was done for two cases, with and without changing density. The observation has shown that the deformation zone is located in the area behind the quartz pipe. The temperature outside the discussed area is much lower because of contact with the tools and existing air-conditioning around the sample (Fig. 4). The deformation zone had the initial height of 30 mm and it was 10 mm in diameter. The sample was subjected to 2 mm reduction. Higher deformation is risky and can lead to damage of the quartz pipe.

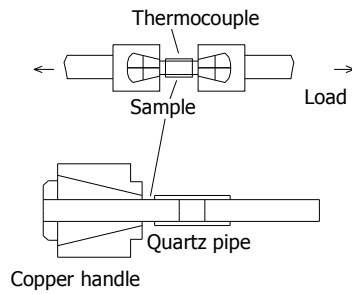


Fig. 4. The scheme of the experimental equipment

Behind the influence of the temperature on the strain and stress fields in the deformation zone, which is rather obvious, the influence of density changes were examined. During computation according to variant no. 1 the density in the deformation zone was assumed to be constant. In opposite during calculations according to variant no. 2 the model with variable density was used.

In Fig. 5 the initial temperature distribution for both the variants is presented. The mean initial temperature in the sample centre was around 1400°C. Taking into account the values of characteristic temperatures one can state the existence of the mushy zone in the sample centre.

The final temperature for the variant no. 2 is shown in Fig. 6. The temperature for the first variant was similar and is not presented in the current paper. All the maps which have ran in the presented contribution concern the upper right quarter of the axial cross-section of the deformation zone.

The analysis of the effective strain fields for specimens no. 1 and no. 2, which are presented in Figs 7 and 8, show that influence of density variations on the metal flow scheme is not very significant, although small differences are clearly visible.

In Figs 9 ÷ 12 stress tensor components are presented. The initial temperature distribution has great influence on the stress field in the deformation zone. The inhomogeneity of the strain field also leads to stress generation. The analysis of the mean stress (Figs. 11 and 12) shows the stress concentration near the upper surface and in the centre of the sample. In accordance with the earlier conjectures for sample no. 2 the stress level is significantly higher than for sample no. 1. In the figures the concentration of the compression stress (negative values) in the sample centre is shown. The stress tensor

components increase with the  $z$  coordinate and at the top reach the positive values (tensile character). The comparison of the constant and variable density models leads to conclusion that in case of changing density the stress components evaluate in tensile state direction. The influence of the density on the stress tensor is important, what is visible in Figs 9 ÷ 12.

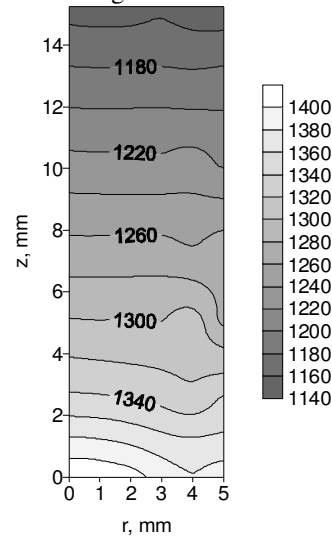


Fig. 5. Initial temperature distribution in the cross-section of the sample – variants 1 and 2

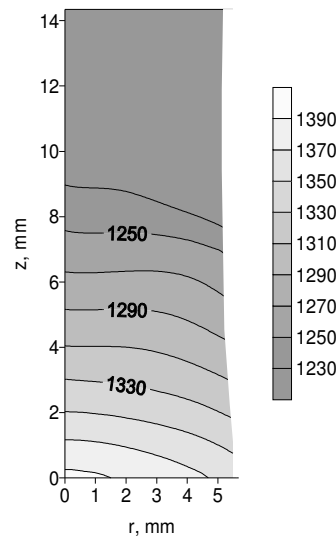


Fig. 6. Final temperature distribution in the cross-section of the sample – variant no. 2

Looking at the stress fields in the controlled volume one can state that the variable density moves the stress tensor components in the tension direction. The stress fields differ significantly for both the variants.

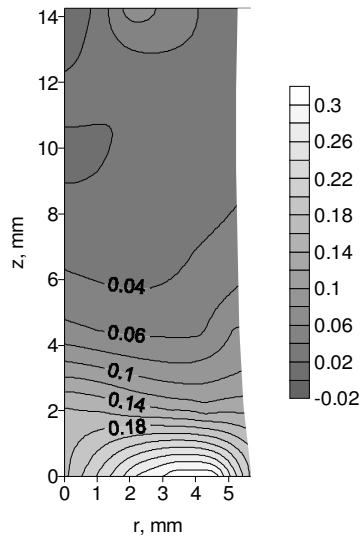


Fig. 7. Effective strain distribution in the cross-section of the sample – variant no. 1

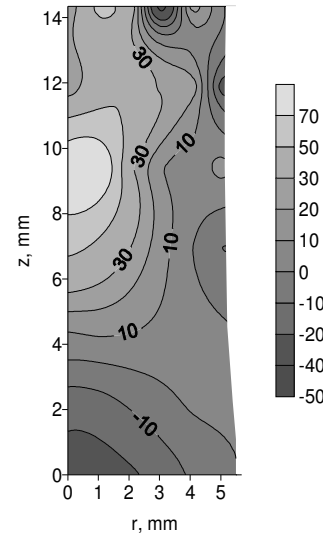


Fig. 9. Radial stress distribution in the cross-section of the sample – variant no. 1

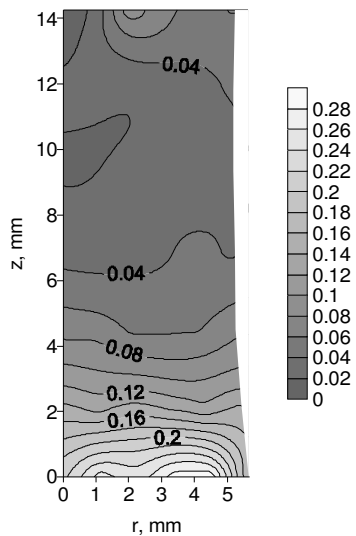


Fig. 8. Effective strain distribution in the cross-section of the sample – variant no. 2

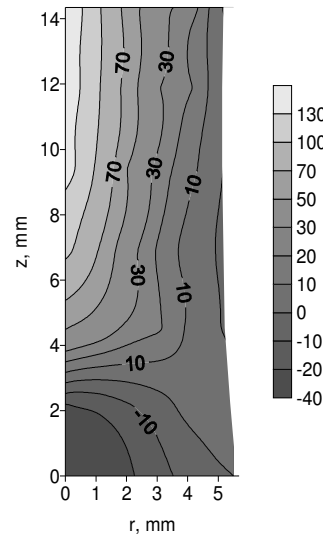


Fig. 10. Radial stress distribution in the cross-section of the sample – variant no. 2

The material properties which have been used in the model are not very accurate because of difficulties in experiment. The existing inhomogeneity of deformation causes problems concerning the calculation of right stress values. The good analysis of the results of experiments needs computer programs to simulate plastic deformation of steel samples. The created model, which takes into account the variable density, can be helpful for the discussed purposes.

## CONCLUSIONS

Modelling of deformation of steel samples with mushy zone requires resolving a few problems,

which are characteristic for the discussed temperature range. One of them is the difficulty in determination of material constants. In aim to know if the deformation is possible in given conditions the computation of characteristic temperatures has to be performed. The most important is the ductility recovery temperature. Plastic deformation in higher temperature is dangerous and can cause damages of the steel specimens. The temperature-dependent, sudden changes of plastic properties of the material require advanced methods of computer simulation of the processes.

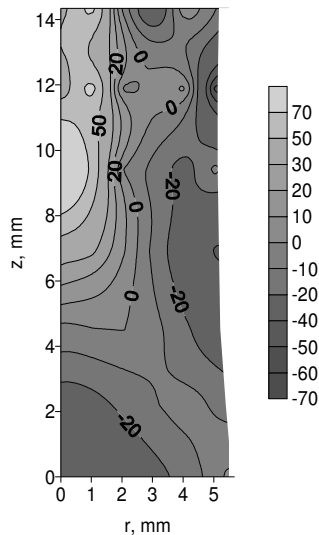


Fig. 11. Mean stress distribution in the cross-section of the sample – variant no. 1

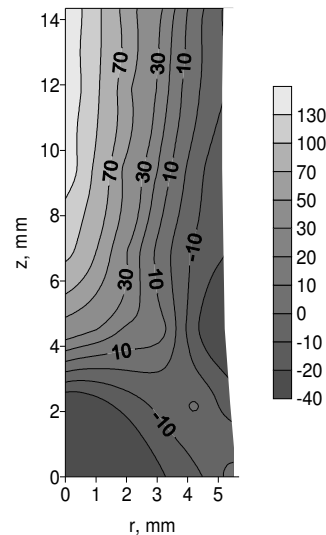


Fig. 12. Mean stress distribution in the cross-section of the sample – variant no. 2

The presented model with incompressibility condition in analytical form allows the simulation of the deformation of material with mushy zone while the material is still changing its state of aggregation. It causes changes of its density. The model can be applied both for bodies with constant or changing density. It allows the simulation of the deformation in conditions which exist during integrated continuous casting and rolling of steel sheets. Numerical form of incompressibility condition causes problems concerning optimisation of the velocity field because of existence of many local minimums and wide flat neighbourhood of the global optimum point.

The presented results are burdened with errors coming from difficulties in calculation of the real strain-stress relationship caused by not exact assessment of the deformation zone limits and inhomogeneity in strain and stress distribution in the zone. The presented model can be very helpful and may allow the right interpretation of results of appropriate tests.

The stress distribution for model without density changes is different in comparison with model taking this phenomenon into account, although the strain distributions are similar in both cases. The stress tensor components calculated according to model with variable density tends toward tensile values.

#### ACKNOWLEDGEMENTS

The financial assistance of KBN is gratefully acknowledged (grant no.:7 T08B 014 20).

#### REFERENCES

1. Suzuki H.G., Nishimura S., Yamaguchi S., Physical simulation of continuous casting of steels, Proc. Physical Simulation of Welding, Hot Forming, and Continuous Casting, Canmet Canada (1988) 1-25
2. Senk D., Hagemann F., Hammer B., Kopp R., Schmitz H.P., Schmitz W., „Umformen und Kühlen von direktgegossenem Stahlband”. Stahl u. Eisen 120, 2000, 65–69
3. Dudek K., Głowacki M., Pietrzyk M., Modelling of stress generated in steels by phase transformation, Proc. Modellierung von Prozessen der Stahlerzeugung und Stahlverarbeitung, eds., D. Janke i R. Kawalla Freiberg, (2000) 230-238. (Freiberger Forschungshefte, B306 Werkstofftechnologie)
4. Głowacki M., Finite element three-dimensional modelling of the solidification of a metal forming charge, J. Mater. Proc. Technol., 60 (1996) 501–504
5. Malinowski Z., The analysis of upsetting with the bending fields method, Doctoral thesis, Kraków 1996.
6. Mizukami H., Yamanaka A., Watanabe T., Prediction of Density of Carbon Steels, ISIJ Int., 42 (2002), No.4, 375-384.
7. Hojny M., Głowacki M., Zalecki W., Strain-stress relationship for steels deformed in extra high temperature, Proc. “Theory and Engineering of Metallurgical Processes”, Kraków 2003, in Polish on CD-ROM.